



Published in final edited form as:

*J Bone Miner Res.* 2017 November ; 32(11): 2182–2193. doi:10.1002/jbmr.3224.

## Kynurenine, a Tryptophan Metabolite that Accumulates with Age, Induces Bone Loss

Mona El Refaey<sup>1,2</sup>, Meghan E. McGee-Lawrence<sup>1,3,5</sup>, Sadanand Fulzele<sup>3</sup>, Eileen J. Kennedy<sup>10</sup>, Wendy B. Bollag<sup>1,3,4,5,6,7,9</sup>, Mohammed Elsalanty<sup>1,7</sup>, Qing Zhong<sup>1,2</sup>, Ke-Hong Ding<sup>1,2</sup>, Nathaniel G. Bendzunas<sup>10</sup>, Xing-ming Shi<sup>1,2,3</sup>, Jianrui Xu<sup>1,2</sup>, William D. Hill<sup>1,3,5,9</sup>, Maribeth H. Johnson<sup>8</sup>, Monte Hunter<sup>3</sup>, Jessica L. Pierce<sup>5</sup>, Kanglun Yu<sup>5</sup>, Mark W. Hamrick<sup>1,3,5</sup>, and Carlos M. Isales<sup>1,2,3,4,5,#</sup>

<sup>1</sup>Institute for Regenerative and Reparative Medicine, Augusta University, Augusta, Georgia, 30912

<sup>2</sup>Department of Neuroscience and Regenerative Medicine, Augusta University, Augusta, Georgia, 30912

<sup>3</sup>Department of Orthopaedic Surgery, Augusta University, Augusta, Georgia, 30912

<sup>4</sup>Department of Medicine, Augusta University, Augusta, Georgia, 30912

<sup>5</sup>Department of Cellular Biology and Anatomy, Augusta University, Augusta, Georgia, 30912

<sup>6</sup>Department of Physiology, Augusta University, Augusta, Georgia, 30912

<sup>7</sup>Department of Oral Biology, Augusta University, Augusta, Georgia, 30912

<sup>8</sup>Department of Biostatistics and Epidemiology, Augusta University, Augusta, Georgia, 30912

<sup>9</sup>Department of Charlie Norwood VA Medical Center, Augusta, Georgia, 30912

<sup>10</sup>Department of Pharmaceutical and Biomedical Sciences, University of Georgia College of Pharmacy, Athens, GA, 30602

### Abstract

Age-dependent bone loss occurs in humans and in several animal species, including rodents. The underlying causal mechanisms are probably multifactorial, although an age-associated increase in the generation of reactive oxygen species has been frequently implicated. We previously reported that aromatic amino acids function as antioxidants and are anabolic for bone and that they may potentially play a protective role in an aging environment. We hypothesized that upon oxidation the aromatic amino acids would not only lose their anabolic effects but also potentially become a catabolic byproduct. When measured *in vivo* in C57BL/6 mice, the tryptophan oxidation product and kynurenine precursor, N-formylkynurenine (NFK), was found to increase with age. We tested the direct effects of feeding kynurenine (kyn) on bone mass and also tested the short-term effects of intraperitoneal kyn injection on bone turnover in CD-1 mice. Micro-CT analyses demonstrated kyn-induced bone loss. Levels of serum markers of osteoclastic activity (PYD and RANKL) increased significantly with kyn treatment. In addition, histological and histomorphometric studies

#Corresponding Author: Carlos M. Isales, MD, Department of Neuroscience and Regenerative Medicine, Augusta University, Augusta, GA 30912. cisales@augusta.edu PH: 706-721-0692 Fax: 706-721-8727.

showed an increase in osteoclastic activity in the kyn-treated groups in both dietary and injection-based studies. Further, kyn treatment significantly increased bone marrow adiposity, and BMSCs isolated from the kyn-injected mice exhibited decreased mRNA expression of Hdac3, and its co-factor NCoR1 and increased expression of lipid storage genes Cidec and Plin1. A similar pattern of gene expression is observed with aging. In summary, our data show that increasing kyn levels results in accelerated skeletal aging by impairing osteoblastic differentiation and increasing osteoclastic resorption. These data would suggest that kyn could play a role in age-induced bone loss.

## Keywords

Bone loss; Indoleamine 2,3 dioxygenase; Aging; Kynurenine

## Introduction

Tryptophan is one of the nine essential amino acids (AA) with several unique features: it is the only amino acid derived from an indole, it is the only amino acid that circulates primarily bound to albumin (85-90% bound/5-10% free) and it is present at the lowest concentration in the blood among the AAs<sup>(1)</sup>. In addition, a number of tryptophan derivatives have significant bioactivity including kynurenine, quinolinic acids, serotonin and melatonin<sup>(2-4)</sup>. Tryptophan is also the main substrate for the *de novo* synthesis pathway for NAD<sup>+</sup>, a key pathway in sirtuin activation and the aging process<sup>(5)</sup>. In fact, tryptophan dietary restriction has been shown to extend rodent lifespan<sup>(6)</sup>. After tryptophan ingestion, this AA can either be utilized for protein synthesis or broken down by various pathways including tryptophan 2,3 dioxygenase (TDO) by cleavage of its indole ring; or indoleamine 2,3 dioxygenase 1 (IDO1) or indoleamine 2,3 dioxygenase 2 (IDO2). IDO1 and IDO2 both catalyze the same reaction but differ in that IDO2 has a much lower affinity for tryptophan than IDO1, though IDO2 may modulate IDO1 activity<sup>(7)</sup>. Kynurenine is the main initial stable metabolic product of the enzymatic breakdown of tryptophan breakdown. TDO is located primarily in the liver and is responsible for the production of most of the kyn in the circulation; in contrast, IDO is expressed in multiple cell types including mesenchymal stem cells and macrophages to regulate local tryptophan breakdown. IDO1 and IDO2 are inducible by inflammation<sup>(8)</sup> primarily by interferon-gamma, and local tryptophan depletion by its breakdown suppresses immune responses<sup>(9,10)</sup>. Interestingly, interferon-gamma activity has been shown to increase with age<sup>(11)</sup> as has IDO activity<sup>(12)</sup>. These findings are consistent with the increase in circulating inflammatory cytokines seen with age (inflamm-aging) and its association with chronic health conditions such as dementia, diabetes and sarcopenia<sup>(13)</sup>. In anabolic states of muscle growth, tryptophan can be used for protein synthesis. However, with increasing age and sarcopenia, the relative contribution of the protein synthesis pathway to tryptophan metabolism decreases<sup>(14)</sup>; the kyn pathway remains a major degradation pathway for tryptophan accounting for 95% of total breakdown. although in general, the liver remains the major site for tryptophan degradation<sup>(15,16)</sup>. IDO1, induced by the associated inflammation seen with aging, becomes the major local tryptophan degradation pathway with generation of kyn as a byproduct. Several metabolites of tryptophan such as kyn and quinolinic acid have been shown to increase with age<sup>(17-19)</sup>,

and these metabolites are implicated in age-related neurodegenerative changes and with increased mortality<sup>(12)</sup>. An increased kynurenine/tryptophan ratio has also been shown to be inversely correlated with bone mineral density (BMD)<sup>(20)</sup>. IDO1 and IDO2 are known to be present in bone marrow mesenchymal stromal cells (BMSCs) and IDO activity is highly inducible by interferon-gamma<sup>(21,22)</sup>. We have previously shown that while tryptophan stimulates BMSC proliferation and differentiation, its metabolite, kyn, can inhibit these anabolic pathways<sup>(23)</sup>.

These previous studies suggested that an elevated kynurenine/low tryptophan environment could contribute to age-induced bone loss by modulating BMSC activity. Therefore, if true, mimicking this “aged” environment in younger mice should also lead to a decrease in bone mass. We attempted to reproduce this environment *in vivo* by restricting dietary protein (lowering tryptophan) and feeding kyn to mature (12-month-old) mice. We found that after eight weeks of low protein/kynurenine feeding, there was significant bone loss and increased marrow adiposity similar to what we have previously reported for aged (24-month-old) C57BL/6 mice<sup>(24)</sup>.

## Materials and Methods

### Measurement of serum kynurenine

Kynurenine and its metabolites were measured by RP-HPLC using a Zorbax SB-C18 column and an Agilent 1200 series HPLC system coupled to an Agilent 6120 quadrupole LC/MS. Serum separation was performed using a 20-minute, 0-100% gradient of acetonitrile containing 0.1% trifluoroacetic acid and water containing 0.1% trifluoroacetic acid. A mass extraction of 236-238 was used to identify N-formylkynurenine. Results are expressed as mAU (milli Absorbance Units). Relative concentrations were determined by injecting equal volumes of undiluted serum extractions for all mice in each age group.

### Generation of kynurenine

For the dietary experiments where kyn was fed to the mice, kyn was synthesized via oxidation of oxindolylalanine as previously described<sup>(23)</sup>. Product formation was monitored by mass spectrometry. Upon completion, the reaction was neutralized to pH 7 by the addition of HCl. Excess solvent was removed by rotary evaporation and kyn purified by solid phase extraction. The product was verified by NMR using a Varian multinuclear 400 MHz NMR spectrophotometer. The purity was assessed and the identity of the product confirmed by mass spectrometry (expected mass=208.2; actual mass=209.1) using an Agilent 1200 HPLC coupled to an Agilent 6120 quadrupole LC/MS. For the kyn injection studies, kyn was purchased commercially (Sigma).

### Animal experimental design

All aspects of the animal research were conducted in accordance with the guidelines set by the Augusta University Institutional Animal Care and Use Committee (AU-IACUC) under a AU-IACUC approved Animal Use Protocol. For low protein and kyn dietary studies, twelve and 24-month-old, male C57BL/6 mice, in groups of 10, were obtained from the aged rodent colony at the National Institute of Aging. The animals were housed individually. 12 and 24-

month-old mice were fed either standard protein (18%) or low protein (8%) diets for eight weeks. Low protein diets were prepared by Harlan-Teklad in consultation with their nutritionist. They were isocaloric purified diets that contained all essential amino acids. For subsequent studies 12-month-old mice were fed one of three specific diets: 1) 18% protein diet (standard protein diet); 2) 8% protein diet + kyn (50  $\mu$ M) and 3) 8% protein diet + kyn (100  $\mu$ M) for 8 wks. Animals were injected with calcein (20 mg/kg) 10 and 3 days prior to euthanasia to label actively mineralizing bone surfaces. The animals were euthanized using CO<sub>2</sub> overdose followed by thoracotomy according to AU-IACUC-approved animal protocols. The animals were weighed at the beginning, at the end and every 2 wks during the experiment. The right femora were fixed in 4% paraformaldehyde (PFA) for 24 hours and then stored<sup>(24)</sup> in 70% ETOH for plastic embedding and histomorphometry. The L4 and L5 vertebrae were fixed in PFA for  $\mu$ CT imaging. Left tibiae were fixed for paraffin embedding and tartrate-resistant acid phosphatase (TRAP) staining.

For kyn injection studies we followed the protocol described by Agudelo et al.<sup>(25)</sup>, with 4-month-old male CD-1 mice obtained from a commercial supplier (Charles River). Mice on standard 18% dietary protein received daily intraperitoneal (i.p.) injections of vehicle (PBS) or L-kynurenine (Sigma # K8625) at 2 or 20 mg/kg bodyweight for 10 days (n=10 per group). No acute adverse effects were detected with either dietary or injected kyn. Mice were injected with calcein (10 mg/kg body weight) on days 5 and 1 before sacrifice. The animals were euthanized using CO<sub>2</sub> overdose followed by thoracotomy according to AU-IACUC-approved animal protocols. Bilateral humerii were collected for BMSC culture. Right tibiae were fixed in 10% formalin and stored in 70% ethanol for plastic embedding and histology.

### Micro-computed tomography ( $\mu$ -CT)

L4 and L5 vertebrae were scanned with an *ex vivo*  $\mu$ -CT system (Skyscan 1174; Skyscan, Aartlesaar, Belgium). The scanner was equipped with a 50 kV, 800  $\mu$ A X-ray tube and a 1.3 megapixel CCD coupled to a scintillator. Samples under examination were maintained in a moist environment to prevent dehydration. Four samples were placed in a plastic sample holder with the long axes oriented parallel to the image plane and scanned in air using 15- $\mu$ m isotropic voxels, 400 ms integration time, 0.5° rotation step, 360° rotation, and frame averaging of 5.

Stacks of two-dimensional X-ray shadow projections were used to reconstruct cross-sectional images using NRecon software (Skyscan), and subjected to morphometric analyses using CTAn software (Skyscan). For three-dimensional (3-D) reconstruction (NRecon software), the grey scale was set from 60 to 140.  $\mu$ -CT images were used for qualitative observations of bone structure and structural parameters were quantified from the  $\mu$ -CT reconstructions. The three-dimensional morphometric parameters of bone micro-architecture were calculated using CTAn (Skyscan) software and the parameters measured include bone volume fraction [bone volume/total volume (BV/TV)], trabecular thickness (Tb.Th) and number (Tb.N).

## Serum assays

Upon euthanasia blood was collected via cardiac puncture, allowed to clot in chilled tubes on ice for approximately 30 min, centrifuged, and the serum separated and stored frozen at  $-80^{\circ}\text{C}$ . Serum assays were performed using an enzyme immunoassay for pyridinoline cross-links (Pyd, a marker of bone breakdown, in particular collagen resorption) (Quidel Corporation, San Diego, CA). The EIA kit recognizes baboon, cat, cow, dog, guinea pig, horse, human, rhesus macaque, mouse, and rat Pyd. A colorimetric kinetic determination of alkaline phosphatase (ALP) activity, a marker of bone formation, was performed using QuantiChrom Alkaline Phosphatase Assay Kit (DALP-250) (BioAssay Systems, Hayward, CA). Serum concentrations of RANKL and OPG were measured using enzyme immunoassay kits (R & D Systems, Inc, Minneapolis, MN).

## Isolation of RNA, synthesis of cDNA, and real-time PCR

Total RNA was isolated from the tibia of mice. Tibia bone particles were ground in liquid nitrogen with a mortar and pestle and the powdered tissue was dissolved in TRIzol. RNA was isolated using the TRIzol method following the manufacturer's instructions, and the quality of the RNA preparations was monitored by absorbance at 260 and 280 nm (Helios-Gamma, Thermo Spectronic, Rochester, NY). The RNA was reverse-transcribed into complementary deoxyribonucleic acid (cDNA) using iScript reagents from Bio-Rad on a programmable thermal cycler (PCR-Sprint, Thermo Electron, Milford, MA). The cDNA (50 ng) was amplified by real-time PCR using a Bio-Rad iCycler and ABgene reagents (Fisher Scientific, Pittsburgh, PA) and appropriate primers (Table 1). Glyceraldehyde-3-phosphate dehydrogenase (GAPDH) was used as the internal control for normalization.

## BMSC culture

For the studies involving BMSC differentiation and mineralization, cells were isolated from the long bones of 6-month-old C57BL/6 mice ( $n=6$ ). The mice were euthanized and the femora and humeri removed. The marrow was then flushed with phosphate-buffered saline (PBS) and the cellular material harvested. The cellular material was then centrifuged, the supernatant discarded and the pellet washed with PBS. The cells were then plated in 100  $\text{cm}^2$  culture plates with DMEM supplemented with 10% heat-inactivated fetal bovine serum (FBS), 50 U/mL penicillin/streptomycin, and 2 mM L-glutamine. After 24 h, the supernatants were removed and the adherent stromal cells trypsinized for negative selection. A negative selection process was used to deplete hematopoietic cell lineages (T- and B-lymphocytic, myeloid and erythroid cells) using a commercially available kit (BD Biosciences), thus retaining the progenitor (stem) cell population. The positive fractions were collected using the following parameters: negative for CD3e (CD3  $\epsilon$  chain), CD11b (integrin  $\alpha\text{M}$  chain), CD45R/B220, Ly-6G and Ly-6C (Gr-1), and TER-119/Erythroid Cells (Ly-76). Next, positive selections were performed using the anti-Stem cell antigen-1 (Sca-1) column magnetic bead sorting kit (Miltenyi Biotec.).

For the studies involving kyn injections in CD-1 mice, humeral shafts were flushed with saline and cells seeded in osteogenic medium (alpha-MEM + 20% FBS + 1% antibiotic/antimycotic, + 50  $\mu\text{g}/\text{mL}$  ascorbic acid + 10 mM beta-glycerophosphate +  $10^{-7}\text{M}$

dexamethasone), as previously described<sup>(26)</sup>. Cells were cultured for 4 days, and total RNA was isolated with TRIzol.

### Alizarin red assay

Alizarin red assays were performed as previously described<sup>(27)</sup>. Briefly, BMSCs (5000 cells/cm<sup>2</sup>) were plated in 24-well plates followed by osteogenic treatment with and without kyn. Alizarin red staining was performed after 21 days. The medium was removed, and the cells washed twice with PBS. The cells were fixed with 70% ethanol for 30 min at 4 °C. The fixed cells were stained with Alizarin red solution (40 mM; 300 µL/well) for 10 min and then washed with PBS until the supernatant was clear. The staining intensity was recorded by photography and the retained dye was extracted with 0.25 mL of 10% (wt/vol) cetylpyridinium chloride solution for 10 min. The solution was diluted at a ratio of 1:10 and read at 570 nm with a spectrophotometer.

### Immunohistochemistry

Samples were processed as previously described<sup>(26)</sup>. Briefly, tibiae were decalcified for 5 days in 15% ethylenediamine tetra-acetic acid (EDTA). Bones were then embedded in paraffin and sectioned at a thickness of 8 µm. Immunohistochemical staining was performed with antibodies directed to Hdac3 (abcam 7030), or an IgG isotype control (Vector Laboratories I-1000). Chromogens were developed using a polyvalent secondary HRP detection kit (Abcam) followed by incubation in DAB (Sigma Aldrich). Sections were counterstained with fast green.

### Histomorphometry for kynurenine dietary and injection studies

The right femora from mice in the dietary studies and the right tibia from mice in the injection studies were prepared for plastic embedding for measurements of dynamic histomorphometry. Bones were fixed in 4% PFA for 24 h and stored in 70% EtOH prior to processing. Bones were dehydrated and embedded in methyl methacrylate and sectioned in the frontal plane at 6–8 µm using a hard tissue microtome. Sections were viewed using an Olympus IX-70 fluorescent microscope to image labeled bone surfaces and section images were captured using a digital camera. Mineralizing surface (MS/BS), bone formation rate (BFR/BV,  $\mu\text{m}^2 / \mu\text{m}^2 \cdot \text{day}$ ) and mineral apposition rate (MAR,  $\mu\text{m}/\text{day}$ ) were calculated as described<sup>(28,29)</sup>.

Left tibiae from the dietary studies were decalcified in 4% EDTA for approximately 2-3 weeks and then dehydrated, cleared in xylene, and embedded in paraffin. Plastic-embedded serial sections from the kyn injection studies were deplasticized in acetone. Sections (5 µm) were stained for tartrate-resistant acid phosphatase (TRAP) activity (Sigma #386A) with either hematoxylin or fast green counterstaining for quantification of osteoclasts or were stained with Goldner's Trichrome for quantification of osteoblasts. Osteoclasts in secondary spongiosa<sup>(30)</sup> were identified by TRAP activity, and osteoclast number (N.Oc/T.Ar, #/mm<sup>2</sup>) and osteoclast surface (Oc.S/BS, %) were quantified with histomorphometry software (Bioquant Osteo, Nashville TN)<sup>(31)</sup>. Adipocyte number (N.Ad/T.Ar, #/mm<sup>2</sup>) and adipocyte volume fraction (AV/TV, %) were quantified from the same sections. Osteoblasts were

identified by morphology, and osteoblast number (Ob.N/BS, #/mm) and osteoblast surface (Ob.S/BS, %) were quantified.

### Statistical analysis

All the data are expressed as mean  $\pm$ SD. Statistical analyses were performed using SAS<sup>®</sup> 9.3 (SAS Institute Inc., Cary, NC). A rank transformation was used prior to analysis where needed to stabilize variance across groups. Differences between the four diet groups were tested using one-way ANOVA. A post-hoc Dunnett's test was used to compare the three supplemented 8% protein groups to the control 18% control diet. The changes from baseline to the 8-week end of study were tested using within diet group paired t-tests. A 4 Diet Group by 5 Week (0, 2, 4, 6, and 8) repeated measures ANOVA was used to test the profile of changes across the study period for body weight. The test of interest was the group by week interaction and a significant interaction would indicate a differential effect of the diets. Significance for all tests was determined at  $\alpha=0.05$ .

## Results

### Aging and Kynurenine Dietary Studies

We speculated that administration of kyn would accelerate skeletal aging. For our initial experiment, then, we monitored the initial tryptophan breakdown product N-formylkynurenine (NFK) in mice of different ages and did, in fact, document that the serum concentrations of NFK were significantly increased with increasing age (Figure 1).

The next set of experiments was designed to determine the impact of dietary protein restriction on bone mass and turnover. We hypothesized that a high kyn, low protein concentration would more closely mimic an aging environment. Thus, initial experiments were first aimed at characterizing the impact of a low protein (8%) diet on bone mass and turnover. Low-protein diets, similar to caloric restriction, have been shown to extend lifespan in mice<sup>(32)</sup>. As shown in Figure 2, in mature mice (12-month) low dietary protein had no impact on bone volume, trabecular number, osteoblast or osteoclast activity. This was in sharp contrast to the negative impact of a low protein diet on bone mass and parameters of bone turnover in the aged mice (24-month; Figure 2). The next experiments were designed to evaluate the impact of addition of increasing concentrations of kyn to 12-month-old mice diets with the purpose of mimicking an aged environment. For these experiments, we placed the mice on a low-protein (8%) diet to minimize the availability of amino acids with antioxidant capacity in order to maximize the pro-oxidant impact of kyn. We elected to supplement the low protein rather than the standard protein diet with kynurenine because a low protein diet has been used as an anti-aging measure<sup>(33)</sup>;

Based on our *in vitro* experiments<sup>(23)</sup>, two concentrations of kyn (50 and 100  $\mu$ m) were selected for dietary studies and added directly to mouse chow prepared by the manufacturer. To ensure that diets did not have a negative impact on overall food intake, body weights at baseline and at 2-week intervals were measured (Tables 2 and 3). At baseline, there was no statistically significant differences in body weight between the different diet groups. We monitored the rate of food consumption between the different groups and found no

statistically significant difference in the amount of food intake (data not shown). For the 18% protein diet, animals showed an increase in body weight at weeks 2, 4, 6 and 8 that was statistically significant ( $p < 0.0001$ ) when compared to baseline. The animals fed the 8% protein containing 50 or 100  $\mu\text{M}$  kyn showed an increase in body weight over time that was statistically significant when compared to baseline. Overall the 8% protein diet groups had lower body weights compared to the 18% dietary protein (Table 3).

We had previously shown that C57BL/6 mice had a total, femoral and spinal bone mineral density (BMD) that peaked at 12 months<sup>(24)</sup> and then remained stable until 18 months of age, decreasing by 24 months. In the present study, however, at the end of eight weeks of dietary intervention in 12-month-old mice, the 8% protein diets containing also 50 or 100 $\mu\text{M}$  kyn negatively impacted bone mass (Figure 3). Bone micro-architecture of L4 and L5 vertebrae was evaluated by  $\mu\text{CT}$ . Bone volume (BV) and bone volume over total volume (BV/TV) were significantly decreased in the 8% protein + 50 $\mu\text{M}$  and 100 $\mu\text{M}$  kyn versus the 18% protein diet (Figure 3A and B). In addition, trabecular number was decreased in the 8% protein + 50 $\mu\text{M}$  kyn (Figure 3C). Trabecular thickness (Fig 3D) tended to be decreased in the kyn-fed group compared to controls but did not achieve statistical significance. To further evaluate the mechanism underlying the kyn-induced decreases in bone mass we next performed bone histomorphometry. Tibial osteoclasts were TRAP-labeled; TRAP-positive osteoclast number, calculated as the number of TRAP-positive osteoclasts per square millimeter of trabecular surface (TRAP+OcN/BS expressed as the no./ $\text{mm}^2$ ) in decalcified tibiae, was significantly increased (3E). Regarding bone formation metrics, although there was a slight decrease in the number of osteoblasts in the 8% protein + 50 $\mu\text{M}$  or 100 $\mu\text{M}$  kyn compared to the 18% protein diet, the values did not achieve statistical significance (Figure 3F). To better visualize these findings we performed 3D reconstructions of representative L4 vertebra of a control mouse (3G) or after feeding 50  $\mu\text{M}$  (3H) or 100  $\mu\text{M}$  (3I) kyn. As shown kyn feeding at either dose resulted in a dramatic decrease in trabecular bone. This was further supported by results from serum markers of bone turnover. The levels of pyridinoline cross-links (PyD), a bone resorption marker, were significantly elevated in the kyn-fed group versus the 18% protein diet (Figure 4A), with an increase of about 50%. This result is consistent with a kyn-induced increase in bone breakdown. No effect of diet on serum alkaline phosphatase activity (a marker of osteoblast activity) was observed (Figure 4B). To further define the mechanism involved in the increase in this marker of bone resorption we measured RANKL (receptor activator of nuclear kappa- $\beta$  ligand) (Figure 4C) a cytokine which promotes osteoclast differentiation, and found it significantly increased after feeding 100  $\mu\text{M}$  kyn. In contrast, levels of osteoprotegerin (OPG), which binds and inactivates RANKL, did not change after kyn feeding (Figure 4D). In terms of dynamic parameters, the mineral apposition rate was decreased in the 8% protein + 50 $\mu\text{M}$  or 100 $\mu\text{M}$  kyn versus the 18% protein diet (Figure 4F) as was the bone formation rate (Figure 4E). These results of increased osteoclastic activity and decreased mineral apposition are similar to the changes seen with aging. Consistent with these findings, kyn feeding resulted in a significant increase in bone marrow adiposity (Figure 6A), with an increase in both adipocyte number and volume. Nutrients are known to induce epigenetic changes, and conditional deletion of histone deacetylase-3 (Hdac3) in the skeleton is known to lead to increased bone marrow adiposity. In addition, Hdac3 activity has been shown to decrease with age and thus



contribute to age-related increases in bone marrow adiposity<sup>(26)</sup>; therefore, we measured Hdac3 expression and found that in fact, kyn decreased expression of Hdac3 in bone as measured by immunohistochemistry (Figure 6B).

### Bone Marrow Stromal Cells and Osteoclasts

Kynurenine results from tryptophan breakdown; thus, we examined both osteoclasts and bone marrow stromal cells for expression of IDO1, the main enzyme responsible for local tryptophan breakdown. We found that osteoclasts strongly express IDO1, while in BMSCs, although IDO1 is clearly present, it is expressed at a lower level than that in osteoclasts (Figure 5A). BMSCs in osteogenic culture respond to kyn treatment with decreased expression of Runx2, a marker of osteoprogenitor commitment (Figure 5B), and in mineralization experiments, kyn also dose dependently inhibited osteoblastic mineralization (Figure 5C).

### Kynurenine Injection Studies

To better define the mechanism by which kyn decreased bone mass, we performed short-term intraperitoneal injection-based studies of kyn's effects on BMSC behavior. To broaden the applicability of our findings we used an outbred mouse strain, CD-1. For these studies we maintained the mice on a standard (18%) dietary protein diet during the kyn injection period. To explore relationships between Hdac3 and marrow adiposity uncovered in the dietary studies, BMSCs were isolated from the kyn-injected mice and cultured; we found that cultures from mice treated with kyn exhibited decreased mRNA expression of Hdac3, similar to what is observed with aging<sup>(26)</sup>. Kynurenine treatment also decreased expression of Hdac3's co-factor NCoR1 and increased expression of the lipid storage genes, Cidec and Plin1, but did not alter the expression of the adipocyte markers Ppar $\gamma$ 2 and Fasn (Figure 6C). A similar pattern of gene expression is observed with both aging and suppression of Hdac3, and suggest that aging-induced increases in bone marrow kyn levels may in fact be responsible for the observed age-related suppression of Hdac3.

Similar to findings with dietary administration of kyn, injection-based kyn administration suppressed bone formation activity, as measured by a significant decrease in bone mineralizing surface (-49%, p=0.018) and a trend for decreased mineral apposition rate (-27%, p=0.09) (Figure 6 D-E). Kynurenine treatment also increased bone resorption activity, as measured by a significant increase in osteoclast number (+760%, p=0.020) (Figure 6F).

### Discussion

Aging is associated with significant changes in multiple organ systems, including bone. In humans, bone mineral density increases until the ages of thirty to thirty-five followed by gradual bone loss of 1-2% after age fifty<sup>(34,35)</sup>. This age-related bone loss is distinct from the bone loss that occurs related to loss of estrogen in women<sup>(36)</sup>. We have previously shown that as BMSCs age, there is a decrease both in their proliferative capacity and in their ability to differentiate into osteoprogenitor cells<sup>(37)</sup>. The mechanisms underlying either age-related bone loss or the decrease in BMSC capacity are poorly understood but may involve

changes in hormonal status, physical activity, circulating levels of inflammatory cytokines or reactive oxygen species (ROS) <sup>(34,38)</sup>. ROS release affects surrounding structural proteins or enzymes resulting in their modification or inactivation <sup>(39,40)</sup>. Individual amino acids can also be oxidized resulting in loss of their anabolic effects on bone cells, but it is not known whether the oxidation products of some of these amino acids might themselves be toxic. Among the 20 amino acid residues, methionine, cysteine, tyrosine and tryptophan are particularly prone to oxidation. Interestingly, these same amino-acids have been implicated in the aging process. To test our hypothesis that oxidation of amino acids with age may produce anti-osteogenic metabolites, we used C57BL/6 mice, since we and others have previously shown that the C57BL/6 mouse is a valid model to study age-induced bone loss <sup>(24,41,42)</sup>. These mice begin to lose bone after 18 months of age and have large drops in bone mass by 24 months of age <sup>(24)</sup>.

The studies presented here demonstrate that while a low-protein diet results in bone loss in aged mice (24-month), it has no impact on bone mass in mature (12-month old) mice. These results are similar to those in a study by Levine et al <sup>(43)</sup> in which the authors report that a low-protein diet impacted body weight in old but not young mice and that high-protein diets were beneficial in aged but not young mice. However, if the tryptophan oxidation product, kyn, is added to the low protein diet or injected, this oxidized AA leads to increased bone resorption, decreased bone formation and a loss of bone mass. Further, kyn injection results in a decrease in Hdac3 expression and an increase in marrow adiposity in a pattern similar to that seen with aging. Of note, for the studies where kyn was administered in the diet (Figure 3), kyn was added to a low protein (8%) diet while the control group was fed a standard protein (18%) diet. The low protein diet was utilized only after our studies showed that by itself a low protein diet did not have a negative impact on bone mass in 12-month-old mice (Figure 2). A limitation of the study was that the control group for Figure 3 was not fed a low protein (8%) diet. However, for the studies where kyn was administered by injection (Figure 6), the mice were fed a standard protein (18%) diet demonstrating that even with the higher protein diet kyn treatment had a negative impact on bone. These data suggest that the detrimental effects seen on bone mass in Figure 2 were related to the kyn and not to the low protein diet.

In view of the fact that kyn is the main metabolic product of tryptophan oxidation and that tryptophan is the essential AA that circulates at the lowest concentrations in humans <sup>(1)</sup>, thus making it particularly susceptible to depletion, our studies focused on kyn. The kynurenine pathway has emerged as a major research focus in immunology, as the depletion of L-tryptophan can have a significant negative effect on cell proliferation, particularly that of T cells <sup>(44,45)</sup>. There are also situations where kyn potentially serves a beneficial function in bone homeostasis. When inflammatory pathways are activated at the tissue level after injury, anti-inflammatory processes are concurrently activated to limit potential damage from unchecked inflammation. This process has best been studied in mouse models of collagen-induced arthritis (CIA) <sup>(46)</sup>, in which injection of type II collagen in mice is used as an animal model for rheumatoid arthritis. CIA results in an increase in the inflammatory cytokine interleukin- $\gamma$ , which stimulates IDO1 expression and the ensuing drop in tryptophan and rise in kyn (which is toxic to T-cells <sup>(46)</sup>) results in a decrease in pro-inflammatory cytokines such as interleukin-17, thus restraining inflammation. As evidence

of this, CIA in IDO1 knockout mice is significantly worse than in control mice <sup>(46)</sup>. Thus, a possible scenario is that age-associated inflammation (inflamm-aging) leads to increased expression of IDO1 and a compensatory increase in kyn. However, in an injury model inflammation is short-lived, whereas with aging, persistently low levels of tryptophan and high levels of kyn, rather than being helpful as anti-inflammatory agents, can themselves become harmful and result in bone loss.

It is also possible that the detrimental effects on bone mass we observed with kyn administration were not due to kyn itself but to other metabolic products. A previous study demonstrated elevated levels of kyn pathway metabolites, such as quinolinic acid and others, in several age-associated conditions and diseases <sup>(47)</sup>. Thus, in this setting, kyn served only as the precursor to these downstream toxic metabolites. These studies are consistent with our hypothesis suggesting a role of kyn in aging; however, whether effects are due solely to kyn is not completely clear.

In contrast to our results, Vidal et al. <sup>(48)</sup> reported that IDO was important for osteoblastogenesis and that IDO1 knockout mice had a low bone mass. The reason for the discrepancy is not clear. It is possible that IDO generates additional metabolites besides kyn, which are anabolic (rather than catabolic) for bone or there might be a dose-dependency to the kyn effect.

In summary, kynurenine treatment of mature (12-month-old) mice results in an increase in osteoclast number and activity, and a decrease in bone formation and bone mass. Kynurenine also decreases the expression of the epigenetic marker, Hdac3, resulting in an increase in marrow adiposity in a pattern similar to that observed with aging (as in 24-month-old mice). These data suggest that age-dependent increases in kynurenine levels might serve as a pathological mediator of age-related bone loss.

## Acknowledgments

This work was supported by a grant from the National Institutes of Aging P01 AG 036675. WBB was supported by a VA Research Career Scientist Award and WDH in part by VA Merit Award 1101CX000930-01. The contents of this article do not represent the views of the Department of Veterans Affairs or the United States Government.

MER, WBB, MWH and CMI were involved in study design, analysis and writing of the manuscript. MEML, SF, EJK, ME, QZ, KHD, NGB, XMS, JX, WDH, JLP, KY were involved in performing experimental procedures. MHJ was involved in data analysis. MH was involved in study design.

## References

1. Badawy AA. Tryptophan availability for kynurenine pathway metabolism across the life span: Control mechanisms and focus on aging, exercise, diet and nutritional supplements. *Neuropharmacology*. 2017; 112(Pt B):248–63. [PubMed: 26617070]
2. Pandi-Perumal SR, BaHammam AS, Brown GM, et al. Melatonin antioxidative defense: therapeutical implications for aging and neurodegenerative processes. *Neurotox Res*. 2013; 23(3): 267–300. [PubMed: 22739839]
3. Reyes Ocampo J, Lugo Huitron R, Gonzalez-Esquivel D, et al. Kynurenines with neuroactive and redox properties: relevance to aging and brain diseases. *Oxid Med Cell Longev*. 2014; 2014:646909. [PubMed: 24693337]
4. van der Goot AT, Nollen EA. Tryptophan metabolism: entering the field of aging and age-related pathologies. *Trends Mol Med*. 2013; 19(6):336–44. [PubMed: 23562344]

5. Srivastava S. Emerging therapeutic roles for NAD(+) metabolism in mitochondrial and age-related disorders. *Clin Transl Med.* 2016; 5(1):25. [PubMed: 27465020]
6. Segall PE, Timiras PS. Patho-physiologic findings after chronic tryptophan deficiency in rats: a model for delayed growth and aging. *Mech Ageing Dev.* 1976; 5(2):109–24. [PubMed: 933560]
7. Metz R, Smith C, DuHadaway JB, et al. IDO2 is critical for IDO1-mediated T-cell regulation and exerts a non-redundant function in inflammation. *Int Immunol.* 2014; 26(7):357–67. [PubMed: 24402311]
8. Brooks AK, Lawson MA, Smith RA, Janda TM, Kelley KW, McCusker RH. Interactions between inflammatory mediators and corticosteroids regulate transcription of genes within the Kynurenine Pathway in the mouse hippocampus. *J Neuroinflammation.* 2016; 13(1):98. [PubMed: 27142940]
9. Majewski M, Kozłowska A, Thoene M, Lepiarczyk E, Grzegorzewski WJ. Overview of the role of vitamins and minerals on the kynurenine pathway in health and disease. *J Physiol Pharmacol.* 2016; 67(1):3–19. [PubMed: 27010891]
10. Palego L, Betti L, Rossi A, Giannaccini G. Tryptophan Biochemistry: Structural, Nutritional, Metabolic, and Medical Aspects in Humans. *J Amino Acids.* 2016; 2016:8952520. [PubMed: 26881063]
11. Oxenkrug G. Interferon-gamma - Inducible Inflammation: Contribution to Aging and Aging-Associated Psychiatric Disorders. *Aging Dis.* 2011; 2(6):474–86. [PubMed: 22396896]
12. Pertovaara M, Raitala A, Lehtimäki T, et al. Indoleamine 2,3-dioxygenase activity in nonagenarians is markedly increased and predicts mortality. *Mech Ageing Dev.* 2006; 127(5):497–9. [PubMed: 16513157]
13. Marttila S, Jylhava J, Eklund C, Hervonen A, Jylha M, Hurme M. Aging-associated increase in indoleamine 2,3-dioxygenase (IDO) activity appears to be unrelated to the transcription of the IDO1 or IDO2 genes in peripheral blood mononuclear cells. *Immun Ageing.* 2011; 8:9. [PubMed: 21989355]
14. Volpi E, Mittendorfer B, Rasmussen BB, Wolfe RR. The response of muscle protein anabolism to combined hyperaminoacidemia and glucose-induced hyperinsulinemia is impaired in the elderly. *J Clin Endocrinol Metab.* 2000; 85(12):4481–90. [PubMed: 11134097]
15. Saito K, Crowley JS, Markey SP, Heyes MP. A mechanism for increased quinolinic acid formation following acute systemic immune stimulation. *J Biol Chem.* 1993; 268(21):15496–503. [PubMed: 8340378]
16. Takikawa O, Yoshida R, Kido R, Hayaishi O. Tryptophan degradation in mice initiated by indoleamine 2,3-dioxygenase. *J Biol Chem.* 1986; 261(8):3648–53. [PubMed: 2419335]
17. Braidy N, Guillemin GJ, Mansour H, Chan-Ling T, Grant R. Changes in kynurenine pathway metabolism in the brain, liver and kidney of aged female Wistar rats. *FEBS J.* 2011; 278(22):4425–34. [PubMed: 22032336]
18. Caballero B, Gleason RE, Wurtman RJ. Plasma amino acid concentrations in healthy elderly men and women. *Am J Clin Nutr.* 1991; 53(5):1249–52. [PubMed: 2021131]
19. de Bie J, Guest J, Guillemin GJ, Grant R. Central kynurenine pathway shift with age in women. *J Neurochem.* 2016; 136(5):995–1003. [PubMed: 26670548]
20. Apalset EM, Gjesdal CG, Ueland PM, et al. Interferon (IFN)-gamma-mediated inflammation and the kynurenine pathway in relation to bone mineral density: the Hordaland Health Study. *Clin Exp Immunol.* 2014; 176(3):452–60. [PubMed: 24528145]
21. Croitoru-Lamoury J, Lamoury FM, Caristo M, et al. Interferon-gamma regulates the proliferation and differentiation of mesenchymal stem cells via activation of indoleamine 2,3 dioxygenase (IDO). *PLoS One.* 2011; 6(2):e14698. [PubMed: 21359206]
22. Meisel R, Zibert A, Laryea M, Gobel U, Daubener W, Dilloo D. Human bone marrow stromal cells inhibit allogeneic T-cell responses by indoleamine 2,3-dioxygenase-mediated tryptophan degradation. *Blood.* 2004; 103(12):4619–21. [PubMed: 15001472]
23. El Refaey M, Watkins CP, Kennedy EJ, et al. Oxidation of the aromatic amino acids tryptophan and tyrosine disrupts their anabolic effects on bone marrow mesenchymal stem cells. *Mol Cell Endocrinol.* 2015

24. Hamrick MW, Ding KH, Pennington C, et al. Age-related loss of muscle mass and bone strength in mice is associated with a decline in physical activity and serum leptin. *Bone*. 2006; 39(4):845–53. [PubMed: 16750436]
25. Agudelo LZ, Femenia T, Orhan F, et al. Skeletal muscle PGC-1 $\alpha$  modulates kynurenine metabolism and mediates resilience to stress-induced depression. *Cell*. 2014; 159(1):33–45. [PubMed: 25259918]
26. McGee-Lawrence ME, Bradley EW, Dudakovic A, et al. Histone deacetylase 3 is required for maintenance of bone mass during aging. *Bone*. 2013; 52(1):296–307. [PubMed: 23085085]
27. Fulzele S, Chothe P, Sangani R, et al. Sodium-dependent vitamin C transporter SVCT2: Expression and function in bone marrow stromal cells and in osteogenesis. *Stem Cell Res*. 2013; 10(1):36–47. [PubMed: 23089627]
28. Dempster DW, Compston JE, Drezner MK, et al. Standardized nomenclature, symbols, and units for bone histomorphometry: a 2012 update of the report of the ASBMR Histomorphometry Nomenclature Committee. *J Bone Miner Res*. 2013; 28(1):2–17. [PubMed: 23197339]
29. Parfitt AM, Drezner MK, Glorieux FH, et al. Bone histomorphometry: standardization of nomenclature, symbols, and units. Report of the ASBMR Histomorphometry Nomenclature Committee. *J Bone Miner Res*. 1987; 2(6):595–610. [PubMed: 3455637]
30. Tang CH, Hsu TL, Lin WW, et al. Attenuation of bone mass and increase of osteoclast formation in decoy receptor 3 transgenic mice. *J Biol Chem*. 2007; 282(4):2346–54. [PubMed: 17099218]
31. Ballanti P, Minisola S, Pacitti MT, et al. Tartrate-resistant acid phosphate activity as osteoclastic marker: sensitivity of cytochemical assessment and serum assay in comparison with standardized osteoclast histomorphometry. *Osteoporos Int*. 1997; 7(1):39–43. [PubMed: 9102061]
32. Le Couteur DG, Solon-Biet S, Cogger VC, et al. The impact of low-protein high-carbohydrate diets on aging and lifespan. *Cell Mol Life Sci*. 2016; 73(6):1237–52. [PubMed: 26718486]
33. Simpson SJ, Le Couteur DG, Raubenheimer D, et al. Dietary protein, aging and nutritional geometry. *Ageing Res Rev*. 2017
34. Curtis E, Litwic A, Cooper C, Dennison E. Determinants of Muscle and Bone Aging. *J Cell Physiol*. 2015; 230(11):2618–25. [PubMed: 25820482]
35. Riggs BL, Melton LJ, Robb RA, et al. A population-based assessment of rates of bone loss at multiple skeletal sites: evidence for substantial trabecular bone loss in young adult women and men. *J Bone Miner Res*. 2008; 23(2):205–14. [PubMed: 17937534]
36. Ucer S, Iyer S, Kim HN, et al. The Effects of Aging and Sex Steroid Deficiency on the Murine Skeleton Are Independent and Mechanistically Distinct. *J Bone Miner Res*. 2016
37. Zhang W, Ou G, Hamrick M, et al. Age-related changes in the osteogenic differentiation potential of mouse bone marrow stromal cells. *J Bone Miner Res*. 2008; 23(7):1118–28. [PubMed: 18435580]
38. Almeida M, O'Brien CA. Basic biology of skeletal aging: role of stress response pathways. *J Gerontol A Biol Sci Med Sci*. 2013; 68(10):1197–208. [PubMed: 23825036]
39. Venditti P, Di Stefano L, Di Meo S. Mitochondrial metabolism of reactive oxygen species. *Mitochondrion*. 2013; 13(2):71–82. [PubMed: 23376030]
40. Brennan LA, Kantorow M. Mitochondrial function and redox control in the aging eye: role of MsrA and other repair systems in cataract and macular degenerations. *Exp Eye Res*. 2009; 88(2):195–203. [PubMed: 18588875]
41. Halloran BP, Ferguson VL, Simske SJ, Burghardt A, Venton LL, Majumdar S. Changes in bone structure and mass with advancing age in the male C57BL/6J mouse. *J Bone Miner Res*. 2002; 17(6):1044–50. [PubMed: 12054159]
42. Glatt V, Canalis E, Stadmeier L, Bouxsein ML. Age-related changes in trabecular architecture differ in female and male C57BL/6J mice. *J Bone Miner Res*. 2007; 22(8):1197–207. [PubMed: 17488199]
43. Levine ME, Suarez JA, Brandhorst S, et al. Low protein intake is associated with a major reduction in IGF-1, cancer, and overall mortality in the 65 and younger but not older population. *Cell Metab*. 2014; 19(3):407–17. [PubMed: 24606898]

44. Alexander AM, Crawford M, Bertera S, et al. Indoleamine 2,3-dioxygenase expression in transplanted NOD Islets prolongs graft survival after adoptive transfer of diabetogenic splenocytes. *Diabetes*. 2002; 51(2):356–65. [PubMed: 11812742]
45. Munn DH, Zhou M, Attwood JT, et al. Prevention of allogeneic fetal rejection by tryptophan catabolism. *Science*. 1998; 281(5380):1191–3. [PubMed: 9712583]
46. Criado G, Simelyte E, Inglis JJ, Essex D, Williams RO. Indoleamine 2,3 dioxygenase-mediated tryptophan catabolism regulates accumulation of Th1/Th17 cells in the joint in collagen-induced arthritis. *Arthritis Rheum*. 2009; 60(5):1342–51. [PubMed: 19404944]
47. Beal MF, Ferrante RJ, Swartz KJ, Kowall NW. Chronic quinolinic acid lesions in rats closely resemble Huntington's disease. *J Neurosci*. 1991; 11(6):1649–59. [PubMed: 1710657]
48. Vidal C, Li W, Santner-Nanan B, et al. The kynurenine pathway of tryptophan degradation is activated during osteoblastogenesis. *Stem Cells*. 2015; 33(1):111–21. [PubMed: 25186311]

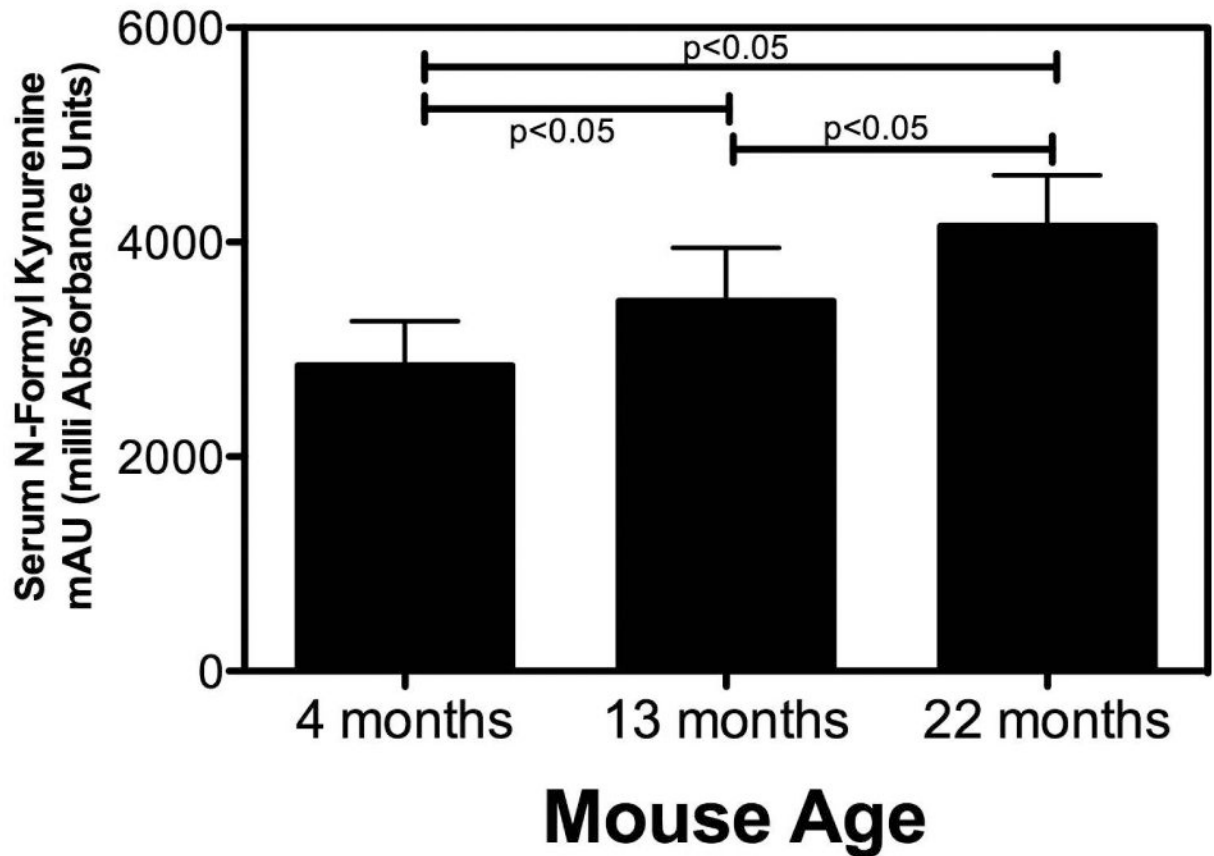


**Figure 1. Serum N-Formylkynurenine Levels Increase with Age**

Mice of the indicated ages were sacrificed and blood collected by cardiac puncture. Serum was prepared and flash frozen in liquid nitrogen. Frozen samples were thawed and analyzed by RP-HPLC for the levels of N-formylkynurenine (NFK) as described in Methods. The units for the MS measurements in the Y-axis are mAU (milli Absorbance Units). Relative concentrations were determined by injecting equal volumes of undiluted serum extractions for all mice of each age group. Values represent the mean  $\pm$  SD of 10 animals of each age.

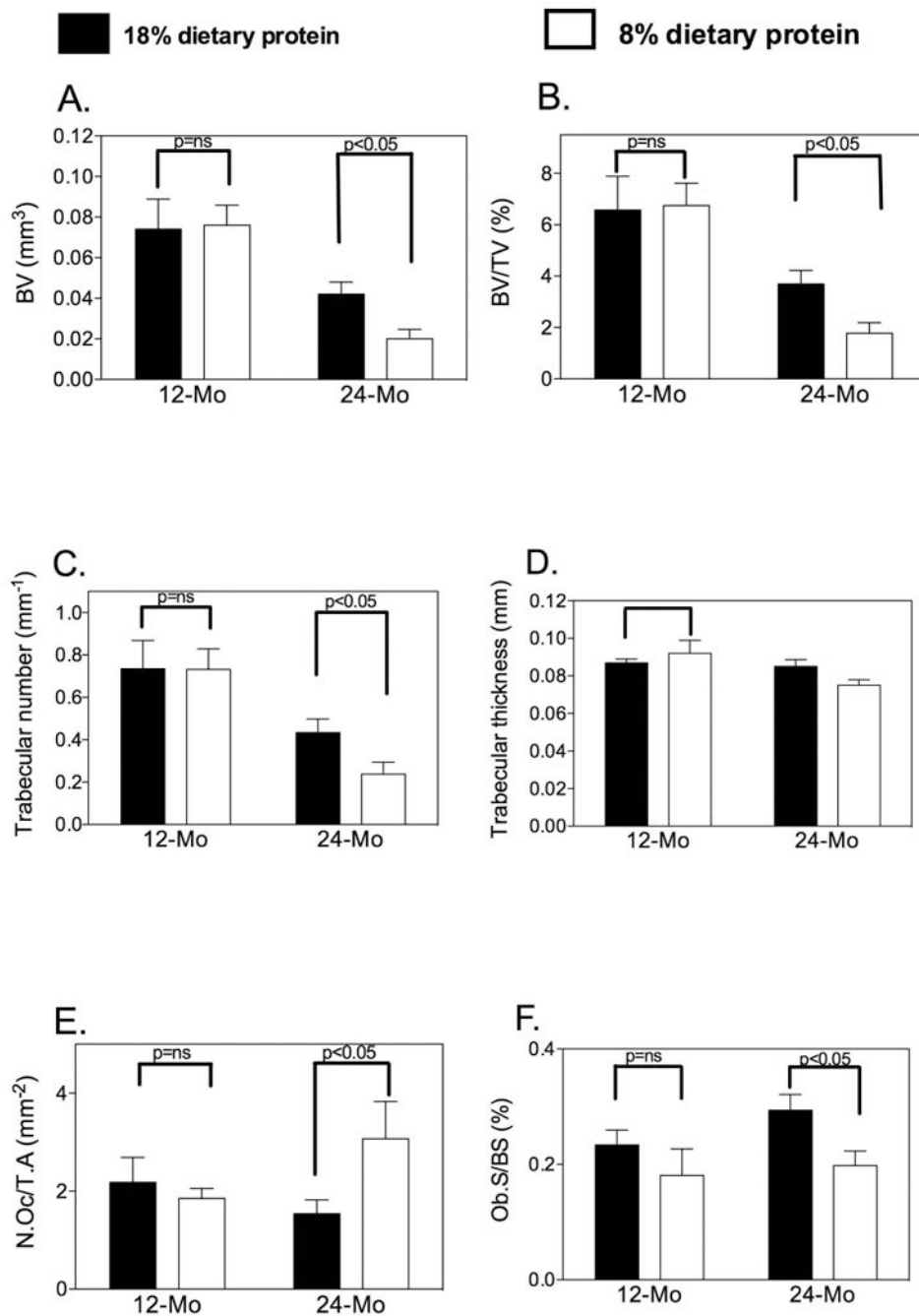


**Figure 2. Bone Microarchitecture in Mature (12-month-old) vs. Aged (24-month-old) Mice after 8 Weeks of Low Dietary Protein Feeding**

Bone microarchitectural parameters of L4 and L5 vertebrae were monitored *ex vivo* by  $\mu$ CT (Skyscan 1174; Skyscan, Aartlesaar, Belgium). (A) Bone volume (in mm<sup>3</sup>) was significantly decreased in the 24-month-old animals fed the 8% protein diet compared to the 18% protein diet. The low dietary protein had no effect on bone mass in the 12-month-old mice; (B) The percentage of bone volume/total volume (BV/TV in %) also showed a statistically significant decrease in the 24-month-old mice fed the 8% protein diet. (C) Trabecular number (Tb.N, per mm) was decreased significantly only in the 24-month old low-protein



animals; (D) Trabecular thickness (in mm) was not altered. (E) Osteoclast number was increased in the 24-month-old mice placed on a low-protein diet while osteoblast number was decreased in this group (F). Data are presented as mean  $\pm$  SD; n=10 for each diet group.

Author Manuscript

Author Manuscript

Author Manuscript

Author Manuscript

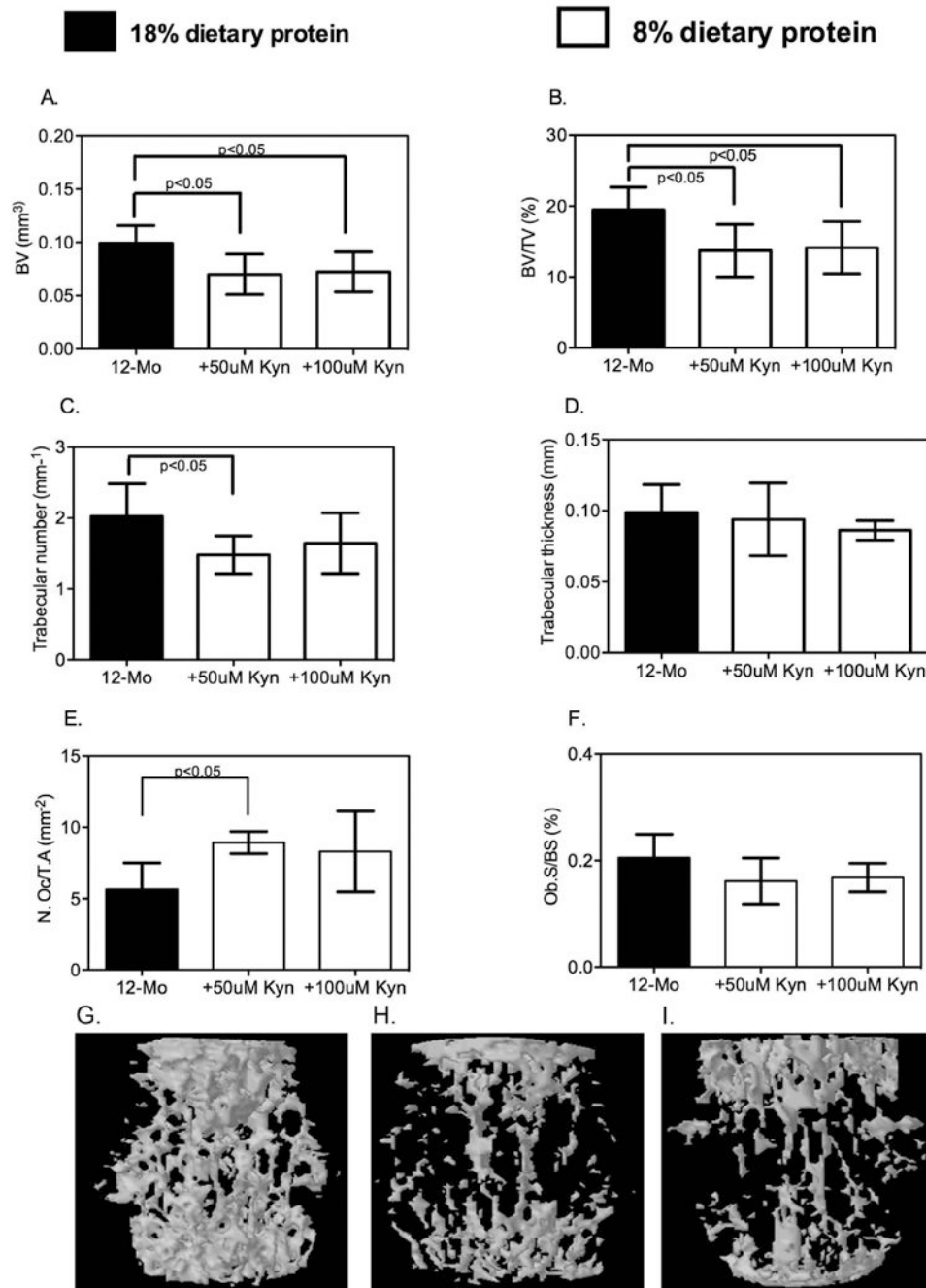


### Figure 3. Bone Microarchitecture is Altered by Dietary Kynurenine Supplementation

Mature (12-month-old) mice were fed the indicated diets and bone microarchitectural parameters of L4 and L5 vertebrae monitored *ex vivo* by  $\mu$ CT. (A) Bone volume (in mm<sup>3</sup>) was significantly decreased in the animals fed the 8% protein diet supplemented with 50 $\mu$ M or 100 $\mu$ M kynurenine compared to the 18% protein diet. (B) The percentage of bone volume/total volume (BV/TV in %) also showed a statistically significant decrease in the kynurenine-supplemented mice versus those fed the 18% protein diet. (C) Trabecular number (Tb.N, per mm) tended to decrease in the kynurenine-supplemented animals; only

the 8% protein + 50 $\mu$ M kynurenine achieved statistical significance. (D) Trabecular thickness (Tb.Th in mm) was not affected. (E) Osteoclast but not (F) osteoblast number was significantly increased by kynurenine. Data are presented as mean  $\pm$  SD; n=9-10 for each diet group, n=5 for osteoclast numbers. Shown in panels G, H and I are representative 3D reconstructions of a vertebra from either a control mouse (3G), or from mice after eight weeks of feeding 50 $\mu$ M kyn (3H) or 100  $\mu$ M kyn (3I).

Author Manuscript

Author Manuscript

Author Manuscript

Author Manuscript

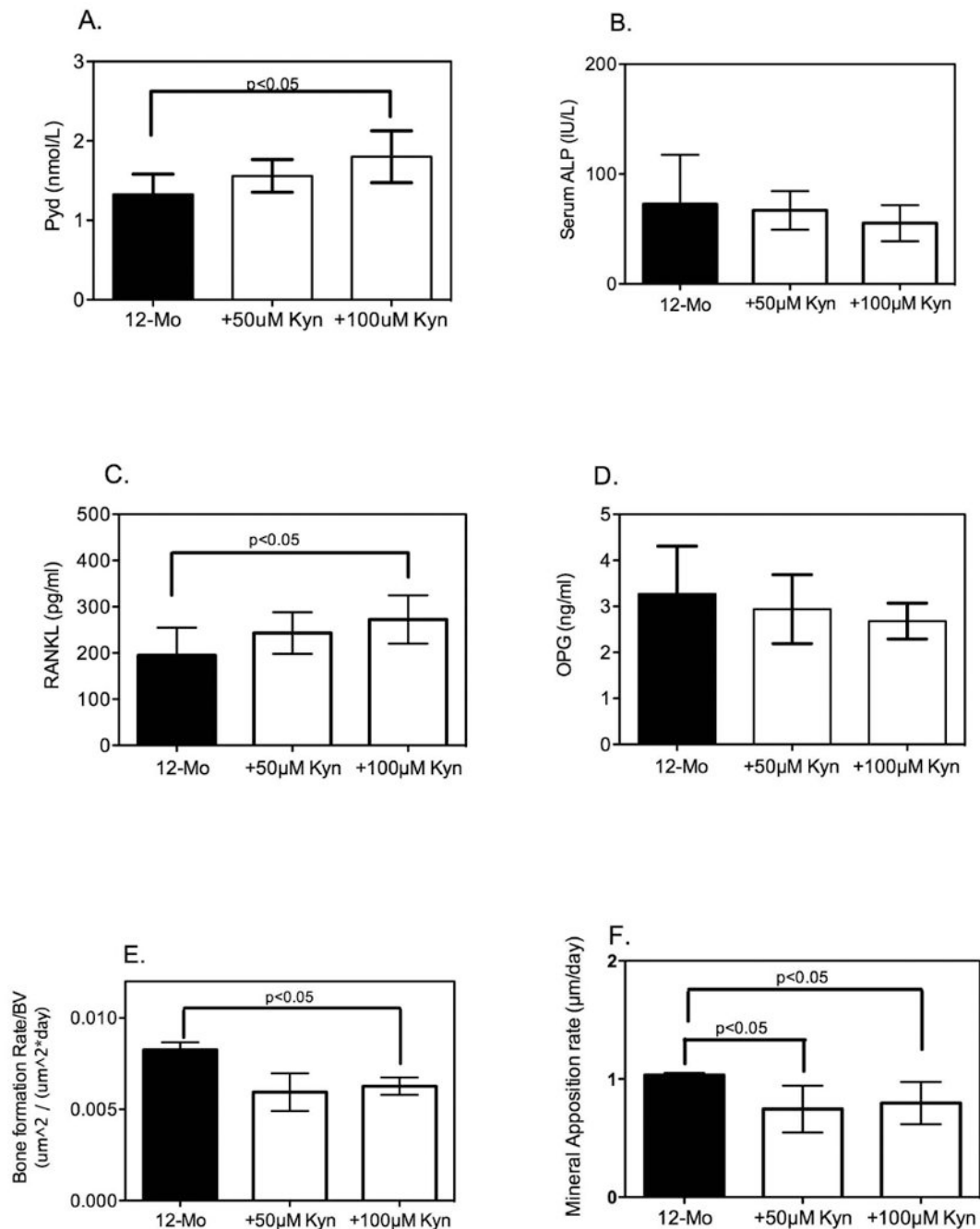


#### Figure 4. Kynurenine Supplementation Increases Bone Breakdown

Serum samples collected from mice fed each diet were assayed as described in Methods. (A) Serum levels of pyridinoline (Pyd) cross-links measured by enzyme immunoassay were increased in the animals fed an 8% protein diet supplemented with kynurenine compared to those fed the 18% protein diet, although only the 8% protein + 100µM kynurenine reached statistical significance. (B) Serum alkaline phosphatase (ALP) activity was monitored by a colorimetric kinetic determination and showed no statistically significant differences among the three diets. Data are presented as mean  $\pm$  SD; n=9 for each group. (C) RANK ligand was

measured by ELISA and was significantly increased at the higher kyn concentration; (D) osteoprotegerin, which binds and inactivates RANKL did not change after kyn feeding. Histomorphometric analysis of femora was performed as described in Methods. (E) Bone formation rates were determined for the three groups and showed a significant decrease with the higher dietary kyn. (F) Mineral apposition rate was measured and found to be significantly decreased in the 8% protein+100 $\mu$ M kynurenine compared to the 18% protein diet. Data are presented as mean  $\pm$  SD.

Author Manuscript

Author Manuscript

Author Manuscript

Author Manuscript

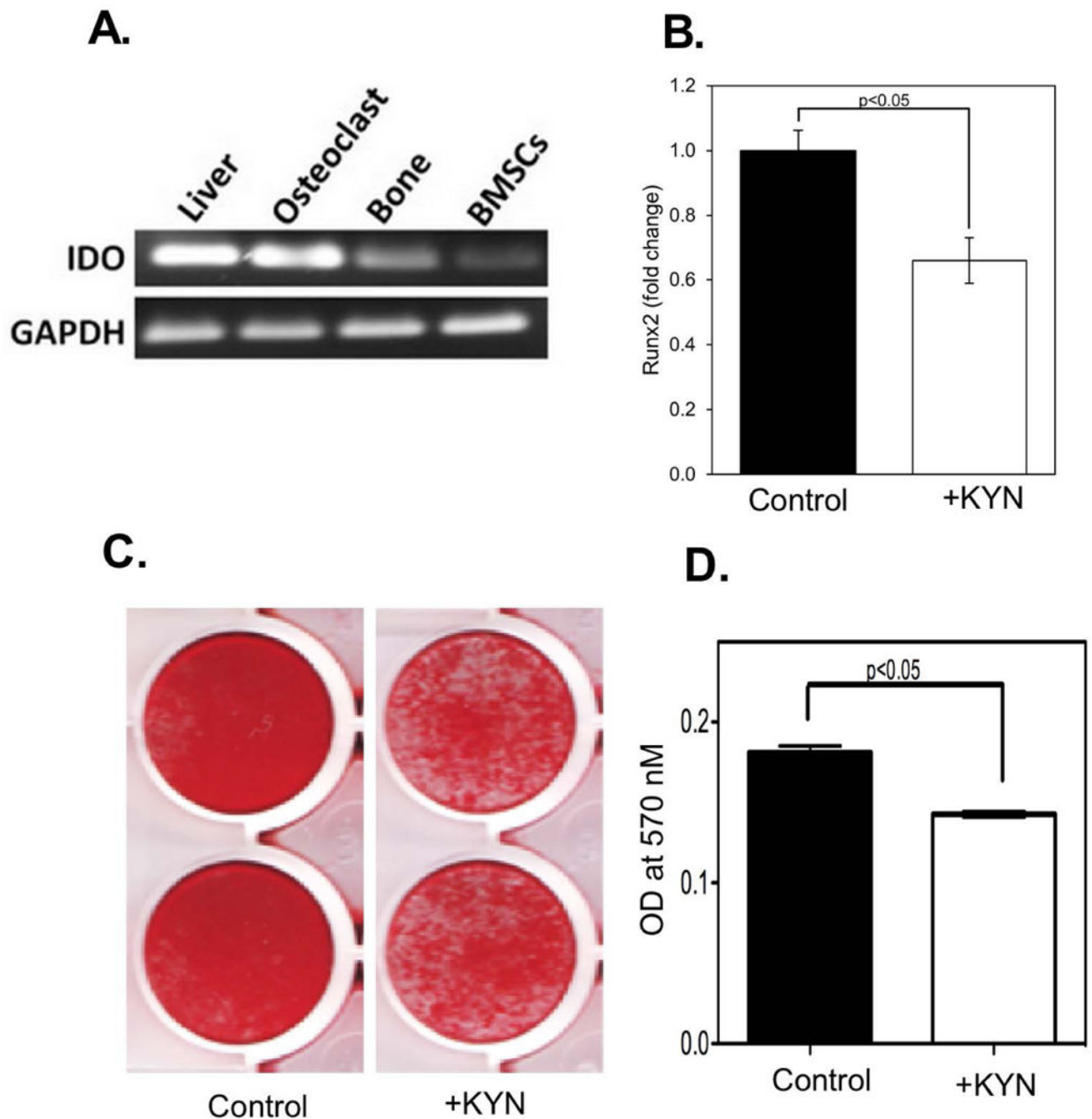


**Figure 5. Indoleamine-2,3-Dioxygenase-1 (IDO1) is Expressed in all Bone Cells and Kynurenine Inhibits BMSC Differentiation and Mineralization**

A) Tissues from C57BL/6 mice were isolated and IDO1 expression determined by RT-PCR with GAPDH measured as the housekeeping control. Shown is a representative experiment, with liver tissue analyzed as a positive control for IDO1 expression. (B) Addition of 100  $\mu$ M kynurenine inhibits the expression of Runx2, a marker of osteoblastic commitment. Data represent the mean  $\pm$  SEM of 3 independent experiments, using BMSC isolated from n = 6 young C57BL6 male mice (3- to 4-months-old) in each experiment on day 7 of osteogenic culture. \* p < 0.05 vs. control; (c) BMSCs isolated from wild-type C57BL/6 were induced to

differentiate using osteogenic medium in the absence and presence of kynurenine (100 $\mu$ M) and bone mineralization determined by alizarin red staining. Results are representative of at least three separate experiments.

Author Manuscript

Author Manuscript

Author Manuscript

Author Manuscript

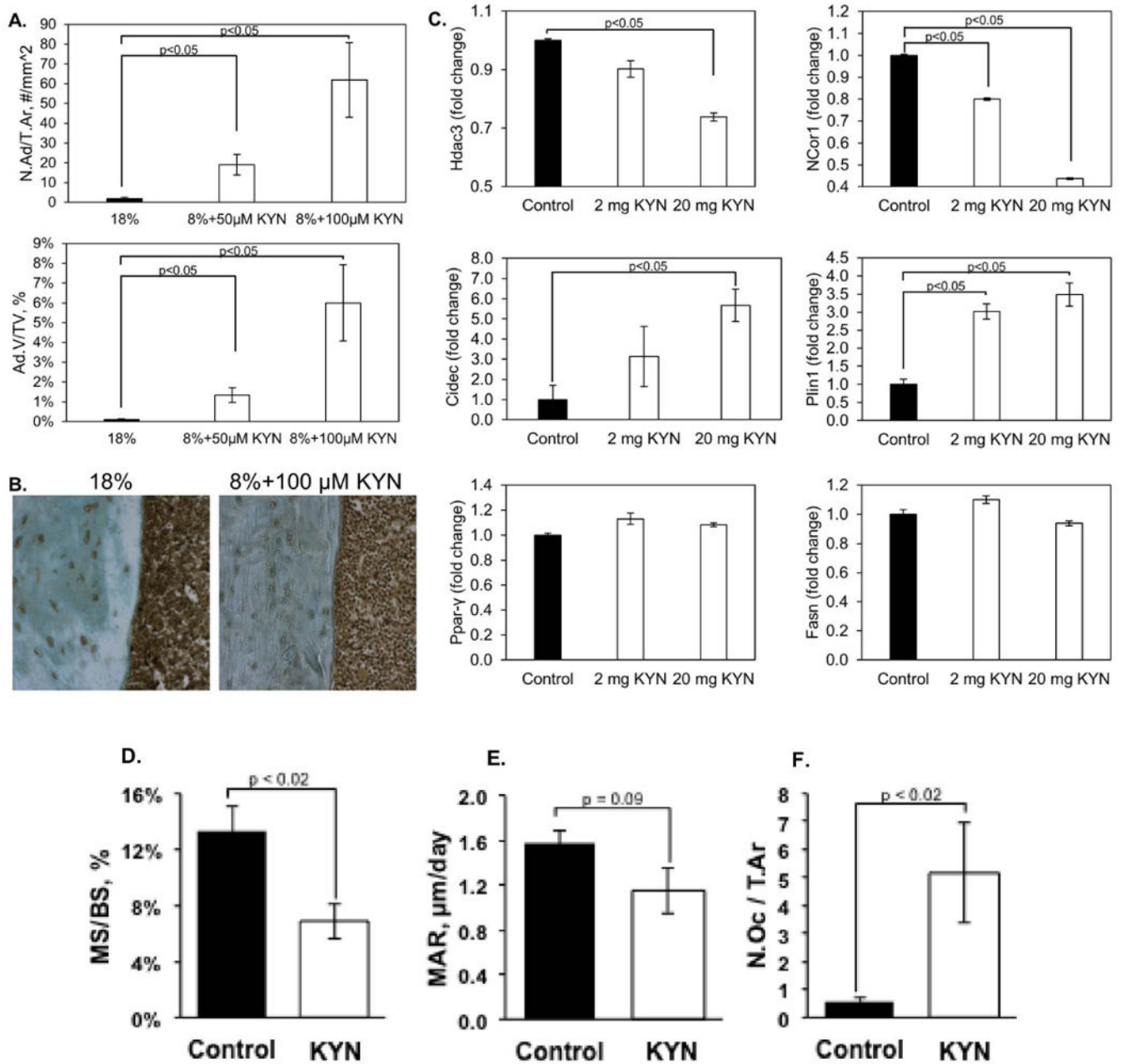


### Figure 6. Kynurenine Supplementation Increases Bone Marrow Adiposity

Tibiae from mice fed the four diets were isolated and the bone marrow analyzed for adiposity as described in Methods. (A) Adipocytes were counted and their volume determined. Values represent the mean  $\pm$  SD, and a dose-dependent increase in both parameters was observed. (B) Representative micrographs of immunostaining for Hdac3 in the cortical bone from the 18% protein group and the 8% protein + 100μM kynurenine. (C) Bone marrow stromal cells were isolated from the humeri of animals injected with kynurenine and the expression of Hdac3 and its cofactor NCoR1, as well as lipid storage genes and adipocyte markers, was determined by quantitative RT-PCR as described in Methods. Values are expressed as means  $\pm$  SEM of n=3. (D-F) Tibiae from mice injected



with vehicle (control) or 20 mg/kg kynurenine were histologically analyzed as described in Methods. Mineralizing surface (D), mineral apposition rate (E), and osteoclast number (F) were quantified. Values represent the mean  $\pm$  SEM of n=5 mice per group.

Author Manuscript

Author Manuscript

Author Manuscript

Author Manuscript

**Table 1**

Primers.

Gene	Primer
IDO	ACTGTGTCCTGGCAAAGTGAAG AAGCTGCGATTCCACCAATAGAG
Runx2	GGAAAGGCACTGACTGACCTA ACAAATTCTAAGCTTGGGAGGA
Cidec	TCCAAGCCCTGGCAAAGAT CGGAGCATCTCCTTCACGAT
Plin1	TGCTGCACGTGGAGAGTAAG TGGGCTTCTTGGTGCTGTT
Fasn	GTGATAGCCGGTATGTCGGG TAGAGCCCAGCCTTCCATCT
Ppary	CCCACCAACTTCGGAATCAG AATGCGAGTGGTCTTCCATCA
Hdac3	GCATTCGAGGACATGGGGAA TTTCGGACAGTGTAGCCACC
Ncor1	TTATCGGAGCCACCTACCCA CAGGTAAGCAGCAGCAGGAT
GAPDH	CATGGCCTCCAAGGAGTAAGA GAGGGAGATGCTCAGTGTGG

Author Manuscript

Author Manuscript

Author Manuscript

Author Manuscript

**Table 2**

Means of body weight of different dietary groups at baseline, every 2 weeks and at the end of the animal experiment (n=10 for each group). Repeated measures ANOVA was performed followed by multiple comparison comparing values at 2, 4, 6 and 8 weeks vs. baseline for each of the groups

Type of diet	Mean body weight Week 0	Mean body weight Week 2	Mean body weight Week 4	Mean body weight Week 6	Mean body weight Week 8
18% protein diet	36.808	39.82 #	43.085 #	45.05 #	45.729 #
8% + 50uM kynurenine	35.364	35.507	37.02 #	38.05 #	38.753 #
8% + 100uM kynurenine	35.575	36.58	38.05 #	39.025 #	38.115 #

# p<0.0001 compared to the value within the group at week 0.

Means of body weights of different dietary groups at baseline, every 2 weeks and at the end of the animal experiment (n=10 for each group). Within week one-way ANOVA data with the three groups of the low-protein diet supplemented with different doses of kynurenine (K) compared to the 18% protein diet at 0, 2, 4, 6 and 8 weeks

**Table 3**

Within Week ANOVA						
Week	0	2	4	6	8	
p-value	0.78	0.0321	0.0033	0.0005	0.0001	
		Dunnett's	Dunnett's	Dunnett's	Dunnett's	Dunnett's
18% protein	36.808	39.82	43.085	45.05	45.729	
8% + 50µM K	35.364	35.507 *	37.02 *	38.05 *	38.753 *	
8% + 100µM K	35.575	36.58	38.05 *	39.025 *	38.115 *	

\* p<0.05 versus the 18% protein group at the same week.